American Journal of MATHEMATICS AND PHYSICS (AJMP)

VOLUME 1 ISSUE 1 (2026)

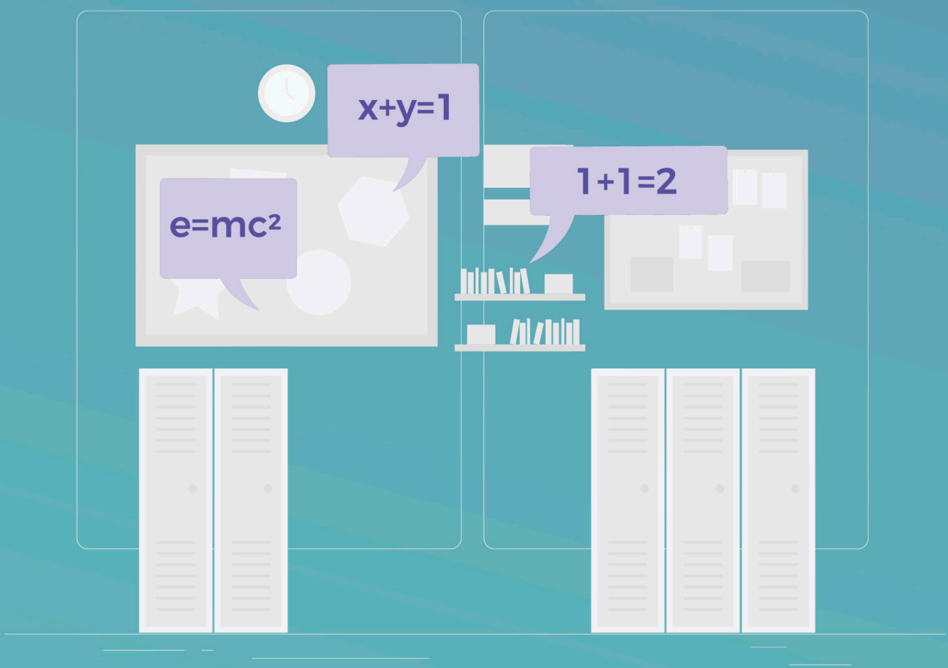

PUBLISHED BY
E-PALLI PUBLISHERS, DELAWARE, USA

American Journal of Mathematics and Physics (AJMP)

Volume 1 Issue 1, Year 2026
DOI: https://doi.org/10.54536/ajmp.v1i1.7687
https://journals.e-palli.com/home/index.php/ajmp

A Matrix Framework for Detuned-Unison Accordion Musette Tuning: Pitch Center, Beat Structure, and Roughness

Giovanni Volpatti[1*]

Article Information

Received: March 09, 2026

Accepted: May 03, 2026

Published: July 03, 2026

Keywords

Accordion Musette, Beat Structure, Detuned Unison, Free-Reed Acoustics, Matrix Formulation, Pitch Center, Roughness

ABSTRACT

Detuned-unison tuning is central to the acoustical behavior of accordion musette, yet its consequences are still described more often qualitatively than through explicit analytical relations. This paper develops a matrix framework for detuned-unison accordion musette tuning that links tuning and balance parameters to three descriptors: beat structure, pitch center, and roughness. Starting from a quasi-harmonic superposition model, the analysis expresses beat-rate sets through pairwise frequency spacings, derives the pitch center as an energy-weighted equivalent frequency, and formulates roughness as a quadratic form that aggregates pairwise interactions across harmonics under auditory weighting. The general relations are then specialized to the two-source and three-source chorus configurations, yielding closed-form expressions that are directly interpretable in terms of detune geometry and reed balance. A deterministic computational pipeline is presented and applied to an accordion case study at 440 Hz with an asymmetric three-reed tuning of −5, 0, and +15 cents. The results show that three-reed musette produces a more complex beat structure than two-reed combinations, that asymmetric detuning can shift the pitch center away from the nominal reference even when one reed is tuned exactly at it, and that roughness depends jointly on the number of interacting pairs, amplitude balance, and harmonic weighting. The proposed framework provides an analytical basis for quantitative comparison, tuning design, and voicing analysis in accordion musette. The study is theoretical and computational, and all reported descriptors are obtained from closed-form relations and a deterministic numerical pipeline.

INTRODUCTION

Detuned-unison tuning is a well-established means of enriching a nominally single pitch by superposing sound sources with small frequency offsets. In accordion practice, this effect is associated with musette tuning, while related phenomena occur in other sustained-tone systems, such as organ celeste ranks. Although the acoustical consequences of such detuning are familiar in practice, tuning design is still described more often through empirical rules, for example target beat rates or dry/wet recipes, than through explicit analytical relations linking tuning and balance parameters to measurable descriptors (Manfredi, 2022; Volpatti, 2025a; Volpatti, 2025b).

Accordion musette provides a particularly suitable setting for a rigorous treatment of detuned unison. When several reeds assigned to the same nominal pitch f_0 are tuned with small offsets around a reference value, the resulting signal exhibits a coupled structure involving pairwise beats, a possible displacement of the effective pitch center, and a degree of roughness determined jointly by detuning, amplitude balance, and spectral content. These features are central to the acoustical identity of musette, yet they are usually discussed separately. A unified formulation is therefore desirable both for physical interpretation and for quantitative comparison of tuning configurations (Causse *et al.,* 1999; Misdariis *et al.,* 2000; Ricot *et al.,* 2005; Llanos-Vazquez *et al.,* 2008; Llanos-Vazquez *et al.,* 2014).

The present work develops a matrix-based analytical framework for detuned-unison accordion musette tuning. The starting point is a quasi-harmonic superposition model of N reeds near a nominal frequency f_0, each characterized by an amplitude and a small detuning. Within this setting, the principal descriptors of interest can be expressed in compact form. Beat structure follows from pairwise frequency separations, pitch center is represented by an energy-weighted equivalent frequency, and roughness is formulated as a quadratic form aggregating pairwise interactions across harmonics under a prescribed spectral weighting. This formulation makes it possible to represent the chorus problem through a small number of algebraic objects while preserving direct physical interpretability (Bader *et al.,* 2019; Cottingham, 1997; Cottingham, 2013).

The general framework is then specialized to the two-source and three-source configurations that dominate practical musette design. This yields explicit closed-form relations showing how the main descriptors depend on detuning geometry and reed balance. In particular, the analysis clarifies that the effective pitch center is not determined solely by the presence of a reed tuned exactly at f_0, but can shift under amplitude asymmetry or asymmetric detuning, and that roughness is intrinsically pairwise, increasing with the number and strength of interacting components. A deterministic numerical

[1] HARMONICUM, Switzerland
[*] Corresponding author's e-mail: giovanni.volpatti@harmonicum.ch

procedure is finally applied to representative accordion musette configurations at 440 Hz in order to obtain reproducible quantitative results (Behrens *et al.,* 2009; Coyle *et al.,* 2009).

The contribution of the paper is therefore twofold. First, it provides a compact analytical framework for detuned-unison musette based on matrix and quadratic-form representations. Second, it demonstrates how this framework can be used to derive, compute, and compare acoustically relevant descriptors for practically meaningful tuning layouts. In this way, the study seeks to place accordion musette tuning on a more explicit quantitative basis, while remaining sufficiently general to support extension to related detuned-unison systems.

LITERATURE REVIEW

Detuned-unison chorus is produced when two or more sustained sources intended to realize the same nominal pitch f_0 are tuned to slightly different frequencies. The resulting sound is well described by a superposition of quasi-harmonic components whose interference introduces a clear separation of time scales. The fast time scale is the carrier oscillation near kf_0 (for harmonic index $k\geq 1$), which largely determines the perceived pitch class and timbral color. The slow time scale is created by small frequency differences between sources, which produces envelope fluctuations and within-band interactions that listeners describe as beating, shimmer, or wetness. The framework developed in this paper is built precisely to exploit this separation: fast carriers are factored out, while the slow dynamics are modeled explicitly through detune-dependent phasors.

At the signal level, the most immediate observable generated by detuned unison is beating. For two sinusoids at frequencies f_1 and f_2, the amplitude envelope contains a modulation component at $|f_1$-$f_2|$. In a chorus cluster with N sources, this generalizes in a strictly pairwise manner: for each pair (i,j) and each harmonic k, the corresponding partials lie near $k(f_0+\delta_i)$ and $k(f_0+\delta_j)$, and their interference introduces a modulation component at the beat rate

$$b_{ij}^{(k)}=k_i|\delta_i\text{-}\delta_j| \tag{1}$$

This scaling with k is central for practical analysis because higher harmonics can contribute substantially to perceived “wetness” even when the fundamental beating is slow. In other words, the same detune pattern can generate a sparse beat structure at low k and a much denser interaction pattern at higher k, depending on how much harmonic energy remains at large k (Plomp & Levelt, 1965; Vencovský, 2016).

A second key ingredient is auditory filtering. Roughness and related interaction sensations are not produced uniformly across the spectrum; they are strongest when partials fall within the same perceptual band, and they diminish when partials are far apart relative to auditory bandwidth. A practical way to represent this bandwidth is the Equivalent Rectangular Bandwidth *(ERB)*, which provides a frequency-dependent scale for auditory resolution. In this paper *ERB* is not introduced as a detailed physiological model; rather, it is used as a widely adopted engineering scale to normalize frequency spacings. In the numerical study we use the standard approximation

so that a spacing Δf can be interpreted relative to a

$$\mathrm{ERB}(f) = 24.7\left(4.37.\frac{f}{1000}+1\right)\ \mathrm{Hz} \tag{2}$$

bandwidth that increases with frequency. This matters because a fixed detune in cents corresponds to a larger spacing in Hz as pitch increases, and because a fixed spacing in Hz can have different perceptual consequences at different f (Moore & Glasberg, 1983; Glasberg & Moore, 1990).

It is also important to distinguish clearly between envelope beating and roughness. Beating refers to slow amplitude modulation that can be perceived as a tremolo-like fluctuation when the modulation rate is low enough and the envelope depth is sufficiently large. Roughness is a different perceptual quality associated with faster within-band interaction of components; it is often described as a dense shimmer or a buzzing texture, and it is typically strengthened by the presence of multiple interacting partial pairs within the same perceptual band. In musette-style chorus, both phenomena can occur simultaneously: the fundamental may produce a clearly countable beat rate, while higher harmonics and multiple pairs may contribute roughness. For this reason the present work treats the beat-rate set as a structural acoustic descriptor of the chorus geometry and introduces a separate scalar KPI R to quantify wetness via an explicitly pairwise interaction model. The roughness KPI is constructed using a kernel $\phi(\Delta f,\bar{f})$ that maps a partial spacing Δf at representative frequency $\bar{f}$ to a nonnegative interaction strength. The analytic development requires only qualitative conditions on ϕ: it vanishes at $\Delta f=0$, increases for small spacings, reaches a maximum at intermediate spacings (relative to bandwidth), and decays to zero for large spacings. The exact parametric choice of ϕ is fixed in the numerical section for reproducibility (Plomp & Levelt, 1965; Vencovský, 2016).

Detuned unison also raises the question of pitch perception. Two notions are relevant and are treated differently in this paper. The first is pitch center (or pitch bias), i.e., the frequency toward which the perceived pitch tends to lean when multiple nearby components are present with unequal strengths. The second is pitch salience (or clarity), i.e., how strongly a single pitch is perceived in the presence of multiple competing components and envelope variability. The framework developed here targets pitch center because it can be derived analytically from the signal model and expressed in closed form as a function of tuning and balance parameters. Pitch salience depends on additional factors such as broadband masking, noise, temporal transients, and auditory grouping, and is therefore not taken as a primary analytic result in this paper; it can be incorporated later as an extension in experimental validation studies or more detailed perceptual modelling.

Finally, it is necessary to state the scope conditions under which the present approach is intended to be used. The main case treated here is detuned-unison chorus in a single perceptual neighborhood, which is the classical musette/celeste situation: multiple sources cluster around the same nominal f_0 and their partials interact predominantly within auditory bands. This regime includes accordion musette and organ celeste ranks directly, and it can also apply to other sustained-tone systems when near-unison components coexist within the same band. There are also important registrations where energy is distributed across widely separated spectral bands, for example octave-spaced combinations or mixtures. In such cases, applying a single-band chorus model globally can mix interactions that are perceptually weak across distant bands. A conservative extension, consistent with the present framework, is to apply the same analysis band-wise: compute the chorus KPIs separately within relevant spectral bands and then combine them through an energy- or loudness-based weighting. This paper keeps the focus on the detuned-unison regime because it is the natural domain of musette and celeste, and because it is precisely where the matrix formulation yields the most direct, interpretable, and design-relevant results.

The present framework is therefore intentionally reduced in scope. It describes the acoustically relevant consequences of small detunings at the signal level and does not attempt a full fluid–structure or aeroacoustic treatment of reed excitation, airflow, pressure-driven nonlinearity, or reed–resonator coupling. These mechanisms are important for sound production and have been examined in dedicated studies of free-reed vibration, airflow interaction, and coupled reed–resonator dynamics; here they are treated as underlying physical processes motivating, but not explicitly resolved within, the present analytical model (Cottingham & Fetzer, 1997; Ricot *et al.,* 2005; Coyle *et al.,* 2009; Bader *et al.,* 2019; Kaufinger *et al.,* 2021).

MATERIALS AND METHODS

Model and Matrix Formulation

This section introduces a unified, instrument-agnostic model for detuned-unison chorus and expresses its main observables in a compact matrix form. The objective is not to reproduce the full physics of reed excitation and airflow, but to derive a tractable signal-level representation of detuned-unison interaction suitable for analytical development and numerical evaluation (Cottingham & Fetzer, 1997; Kaufinger *et al.,* 2021; Volpatti, 2024a; Volpatti, 2026a; Volpatti, 2026b). The formulation is constructed to separate the fast carrier oscillation at the nominal pitch from the slow dynamics induced by small detunes, to make the beat structure explicit, and to yield closed-form expressions for a pitch-center estimator and a roughness ("wetness") functional (Carpinteri & Accornero, 2021; Davolio *et al.,* 2023; Volpatti *et al.,* 2022; Volpatti, 2024e; Volpatti, 2025c; Volpatti, 2025d; Volpatti, 2025e; Volpatti, 2025f; Volpatti, 2025g). Throughout, scalars are written plainly (e.g., f_0), vectors use curly braces `` (e.g., `a`), and matrices use square brackets `[]` (e.g., `[D]`). Transpose is $(\cdot)^\top$. The imaginary unit is $j=\sqrt{(-1)}$.

Consider N sources intended to realize the same nominal *pitch* $f_0>0$. *Source* $i\in 1,\ldots,N$ *has a fundamental frequency* f_i and is represented by two parameters: a detune δ_i in Hz relative to f_0, and an amplitude $A_i\geq 0$. Thus,

$$f_i=f_0+\delta_i \tag{3}$$

If detuning is specified in cents c_i, then and let $1=1,\ldots,1^\top$ denote the all-ones vector of length N.

$$f_i = f_{0,}2^{c_i/1200}, \qquad \delta_i = f_i - f_0 = f_0\left(2^{c_i/1200}-1\right) \tag{4}$$

Define the amplitude vector and detune matrix

$$a = A_1, \ldots, A_N{}^\top, \qquad [D] = \mathrm{diag}(\delta_1, \ldots, \delta_N), \tag{5}$$

The signal is modelled as quasi-harmonic. A common harmonic envelope $E_k\geq 0$ is used to describe the relative strength of harmonic k (for $k=1,\ldots,K$), and an optional perceptual weight $w_k\geq 0$ may be used when aggregating quantities across harmonics. The analysis below is first written with generic E_k and w_k; particular choices are part of the numerical protocol.

A key step is to separate the fast carrier oscillation at kf_0 from the slow chorus dynamics caused by detuning. The real signal is written as where $S_k(t)$ is a complex baseband sum that evolves slowly compared with $e^{(j2\pi k f_0 t)}$. Define

$$s(t) = \sum_{k=1}^{K}\mathrm{R}\{e^{j2\pi k f_0 t}\ S_k(t)\} \tag{6}$$

the slow phasor vector

$$u_k(t)=e^{((j2\pi k[D]t))}\ 1 \tag{7}$$

Because $[D]$ is diagonal, $e^{((j2\pi k[D]t))}$ is diagonal with entries $e^{(j2\pi k\delta_i t)}$. Hence,

$$u_k(t) = e^{j2\pi k\delta_1 t}, \ldots, e^{j2\pi k\delta_N t}{}^\top \tag{8}$$

This representation isolates tuning geometry in $[D]$ and The baseband sum at harmonic k is then the scalar

$$S_k(t) = E_k a^\top u_k(t) = E_k\sum_{i=1}^{N} A_i e^{j2\pi k\delta_i t} \tag{9}$$

registration balance in $\{a\}$.

The beat structure is most transparent in the squared *magnitude* $|S_k(t)|^2$, which represents the instantaneous baseband power of harmonic k. Expanding yields a quadratic form governed by a cosine interference matrix.

Proposition 1 (Envelope quadratic form)

For each harmonic (k),

$$|S_k(t)|^2=E_k^2\, a^T\, [J_k(t)]a \tag{10}$$

where $[J_k(t)]\in\mathbb{R}^{(N\times N)}$ is defined entrywise by

$$[J_k(t)]_{ij}=\cos(2\pi k(\delta_i-\delta_j)t) \tag{11}$$

Proof. From the definition, Taking the real value (the expression is real by construction) gives

A direct consequence is that modulation components are pairwise. For each pair (i,j), the cosine term oscillates at

$$S_k(t) = E_k\sum_{i=1}^{N} A_i e^{j2\pi k\delta_i t}, \tag{12}$$

$$S_k^*(t) = E_k\sum_{j=1}^{N} A_j e^{-j2\pi k\delta_j t} \tag{13}$$

Therefore,

$$|S_k(t)|^2 = S_k(t)S_k^*(t) = E_k^2\sum_{i=1}^{N}\sum_{j=1}^{N} A_i\, A_j e^{j2\pi k(\delta_i-\delta_j)t} \tag{14}$$

$$|S_k(t)|^2 = E_k^2 \sum(i=1)^N \sum(j=1)^N A_i A_j \cos(2\pi k(\delta_i - \delta_j)t) = E_k^2 a^T [J_k(t)] a \quad (15)$$

the beat rate

$$b_{ij}^{(k)} = k, |\delta_i - \delta_j| \quad (16)$$

Thus, the complete beat-rate architecture is determined by detune differences encoded by *[D]*.

The same framework yields a closed-form pitch-center estimator. Detuned unison raises the question of where the perceived pitch "leans" when multiple nearby fundamentals coexist. Here, pitch center is defined as an energy-weighted average instantaneous frequency of the analytic signal associated with the fundamental-band cluster. This definition is time-domain and physically grounded, yet it yields a simple expression in terms of *[D]* and $\{a\}$ under a mild averaging condition.

Define the fundamental-band baseband sum (carrier f_0 removed):

$$Z(t) = \sum_{(i=1)}^{N} A_i e^{(j2\pi\delta_i t)} \quad (17)$$

The analytic signal of the fundamental-band cluster is

$$z(t) = e^{(j2\pi f_0 t)} Z(t) \quad (18)$$

Define the instantaneous frequency of z(t) by

$$f_{inst}(t) = 1/2\pi \ d/dt \ \arg \boxed{f0} z(t) \quad (19)$$

Because $z(t)=e^{(j2\pi f_0 t)} Z(t)$, the carrier separates:

$$f_{inst}(t) = f_0 + 1/2\pi \ d/dt \ \arg \boxed{f0} Z(t) \quad (20)$$

Introduce the time-average operator over a window of length T,

$$\langle g \rangle_T = 1/T \int_0^T g(t) \ dt \quad (21)$$

and define an energy-weighted pitch-center estimate over [0,T] as

$$f_{eq}(T) = \langle |Z(t)|^2 f_{inst}(t) \rangle_T / \langle |Z(t)|^2 \rangle_T \quad (22)$$

Assume T is large relative to the inverse of all nonzero detune differences so that oscillatory cross terms average to zero:

$$T \gg 1/|\delta_i - \delta_j| \text{ "for all " } i \neq j \text{" with " } \delta_i \neq \delta_j \quad (23)$$

A standard identity for complex signals gives

$$d/dt \ \arg \boxed{f0} Z(t) = (\text{"Im" } Z^*(t) \dot{Z}(t)) / |Z(t)|^2 \quad (24)$$

$$\dot{Z}(t) = dZ/dt \quad (25)$$

Hence,

$$|Z(t)|^2 (f_{inst}(t) - f_0) = (1/(2\pi)) \mathrm{Im}(Z^*(t) dZ(t)/dt) \quad (26)$$

Averaging both sides and dividing by $\langle |Z(t)|^2 \rangle_T$ yields

$$f_{eq}(T) = f_0 + 1/2\pi \ \langle \text{"Im" } Z^*(t) \dot{Z}(t) \rangle_T / \langle |Z(t)|^2 \rangle_T \quad (27)$$

It remains to compute the two time averages. First,

$$\dot{Z}(t) = \sum_{(i=1)}^{N} A_i , j2\pi\delta_i , e^{(j2\pi\delta i \ t)} \quad (28)$$

Then

$$Z^*(t)\dot{Z}(t) = j2\pi \sum_{i=1}^{N} \sum_{j=1}^{N} A_i A_j \delta_i , e^{j2\pi(\delta_i - \delta_j)t} \quad (29)$$

and therefore

$$\mathrm{Im}\, Z^*(t) Z(t) = 2\pi \sum (i=1)^N \sum (j=1)^N A_i A_j \delta i \cos(2\pi(\delta_i - \delta_j)t) \quad (30)$$

Under the averaging condition, only the i=j terms have nonzero mean, giving

$$\mathrm{Im}\, Z^*(t) \dot{Z}(t) \rangle_T \longrightarrow 2\pi \sum_{(i=1)}^{N} A_i^2 \ \delta_i \quad a\text{" "} T \to \infty \quad (31)$$

$$|Z(t)|^2 = \sum(i=1)^N \sum(j=1)^N A_i A_j \cos(2\pi(\delta_i - \delta_j)t) \Rightarrow \langle |Z(t)|^2 \rangle_T \to \sum(i=1)^N A_i^2 \, as T \to \infty \quad (32)$$

Similarly,

Theorem 1 (Pitch center; Rayleigh quotient)

$$f_{\mathrm{eq}} = \lim_{T\to\infty} f_{\mathrm{eq}}(T) = f_0 + \frac{\sum_{i=1}^{N} A_i^2 \delta_i}{\sum_{i=1}^{N} A_i^2} = f_0 + \frac{a^\top [D] a}{a^\top a} \quad (33)$$

Under the above averaging condition,

This result is exact in Hz and makes the dependence on detuning geometry and balance explicit. In particular, pitch center is determined by a power-weighted detune moment and can therefore shift under asymmetric tuning and/or unequal balance even if a "reference" source exists at $\delta=0$.

In many practical contexts, pitch judgments may be influenced by higher harmonics and by auditory weighting. A convenient aggregated pitch-center estimator is obtained by combining harmonic contributions with weights w_k and envelopes E_k. Applying the same reasoning

$$f_e q^{(w)} = f_0 + (\sum(k=1)^K w_k E_k^2 k \, a^T [D] a) / (\sum(k=1)^K w_k E_k^2 a^T a) \quad (34)$$

band-wise gives the weighted estimate

This expression preserves the same structural dependence on *[D]* and $\{a\}$ while allowing controlled emphasis of particular harmonic bands.

To model wetness, a scalar beat-rate description is not sufficient, because roughness depends on within-band interaction of multiple partial pairs and on harmonic energy distribution. The present approach defines a roughness functional that is explicitly pairwise, harmonically aggregated, and expressible as a quadratic form.

Let $\phi(\Delta f, \bar{f}) \geq 0$ be a kernel mapping a spacing Δf at representative frequency $\bar{f}$ to an interaction strength. For the analysis below it is sufficient that $\phi(0,\bar{f})=0$, that ϕ increases for small Δf, reaches a maximum at intermediate spacing (relative to auditory bandwidth), and decays to zero as $\Delta f \to \infty$. For harmonic k, the spacing between the k-th harmonics of sources i and j is $k|\delta_i - \delta_j|$, and the representative frequency is taken as kf_0. Define the

$$G_i i = 0, \ G_i j = \sum(k=1)^K E_k^2 \varphi(k|\delta_i - \delta_j|, \ kf_0) \ (i \neq j) \quad (35)$$

symmetric coupling matrix $[G] \in R^{(N\times N)}$ by

The interpretation is direct: G_{ij} aggregates, over harmonics, the interaction strength of the pair (i,j), shaped by the harmonic envelope E_k.

Define total roughness R as the sum of pairwise contributions weighted by amplitude products:

$$R = \sum_{(1\leq i<j\leq N)} A_i \ A_j \ G_{ij} \quad (36)$$

Proposition 2 (Quadratic-form roughness)

With [G] defined above,

$$R = 1/2 a^T [G] a \quad (37)$$

$$a^\top [G] a = \sum_{i=1}^{N} \sum_{j=1}^{N} A_i G_{ij} A_j = \sum_{i\neq j} A_i G_{ij} A_j = 2 \sum_{i<j} A_i G_{ij} A_j = 2R \quad (38)$$

Proof. Since $G_{ii}=0$ and [G] is symmetric,

Hence $R=1/2 a^T [G]a$.

Two features are immediate. First, $R \geq 0$ by construction. Second, roughness is intrinsically pairwise and accumulative: it sums contributions from every source pair (i,j), each shaped by detune spacing, pitch, and harmonic weighting.

The quadratic forms above also yield simple sensitivity expressions useful for tuning and voicing analysis. For

$$p = a^\top a = \sum_{i=1}^{N} A_i^2 \,,\ q = a^\top [D] a = \sum_{i=1}^{N} A_i^2\, \delta_i,\ \bar{\delta} = \frac{q}{p} \quad (39)$$

Then $f_{\text{eq}} = f_0 + \bar{\delta}$), and differentiation gives

$$\frac{\partial f_{\text{eq}}}{\partial A_i} = \frac{\partial}{\partial A_i}\left(\frac{q}{p}\right) = \frac{2A_i\delta_i, p - 2A_i q}{p^2} = \frac{2A_i(\delta_i - \bar{\delta})}{p} = \frac{2A_i(\delta_i - \bar{\delta})}{a^\top a} \quad (40)$$

pitch center, define

Thus, increasing the amplitude of a source with $\delta_i > \bar{\delta}$ increases the pitch center, while increasing the amplitude of a source with $\delta_i < \bar{\delta}$) decreases it.

For roughness, since $R = 1/2\, a^T [G] a$ and $[G]$ is symmetric and independent of $\{a\}$ for fixed detunes and envelopes, the gradient is

$\nabla_a R = [G] a$ equivalently $\partial R / (\partial A_i) = ([G]a)_i$ (41)

This provides a direct quantitative measure of how each source's amplitude affects wetness given the detune geometry and harmonic weighting.

The next section specializes these general results to the two-source and three-source cases, expanding the matrix relations into explicit expressions for beat components, pitch-centering conditions, and roughness decomposition into physically interpretable pair contributions.

Closed-form Specializations

This section specializes the general matrix relations to the two configurations that dominate practical detuned-unison work: two-source chorus and three-source chorus. The objective is to provide explicit formulas that are directly verifiable, simple to implement, and interpretable in terms of tuning geometry and balance. The results are purely analytic; numerical values are introduced later in the case study.

Consider first a two-source cluster with detunes δ_1, δ_2 and amplitudes A_1, A_2. The harmonic-k baseband sum is

$S_k(t) = E_k\,(A_1\, e^{(j2\pi k\delta_1 t)} + A_2\, e^{(j2\pi k\delta_2 t))}$ (42)

Expanding the squared magnitude gives the exact

$$|S_k(t)|^2 = E_k^2\left(A_1^2 + A_2^2 + 2A_1A_2 cos(2\pi k(\delta_1 - \delta_2)t)\right) \quad (43)$$

envelope power

Thus, two-source chorus has one modulation component per harmonic, with beat rate

$b_{12}^{(k)} = k|\delta_1 - \delta_2|$ (44)

A convenient modulation-depth indicator can be defined

$$M_k = \frac{|S_k|_{max}^2 - |S_k|_{min}^2}{|S_k|_{max}^2 + |S_k|_{min}^2} \quad (45)$$

from the squared envelope by

$cos(\cdot) = \pm 1$, yielding (46)

$$|S_k|_{max}^2 = E_k^2(A_1 + A_2)^2,\ |S_k|_{min}^2 = E_k^2(A_1 - A_2)^2$$

and therefore

$$M_k = \frac{(A_1+A_2)^2 - (A_1-A_2)^2}{(A_1+A_2)^2 + (A_1-A_2)^2} = \frac{2A_1A_2}{A_1^2 + A_2^2} \quad (47)$$

This expression depends only on balance, not on detune. Detune controls the modulation rate, whereas balance controls the modulation depth; the depth reaches its maximum when $A_1 = A_2$ and decreases as the amplitudes become unequal.

The pitch center for two sources follows from Theorem 1: (48)

$$f_{\text{eq}} = f_0 + \frac{A_1^2\delta_1 + A_2^2\delta_2}{A_1^2 + A_2^2}$$

In the symmetric detune case $\delta_1 = -\delta$, $\delta_2 = +\delta$ with equal power $A_1 = A_2$, the pitch center locks exactly at f_0, whereas power imbalance shifts the pitch center toward the stronger source. The roughness coupling reduces to a single pair coefficient (49)

$$G_{12} = \sum(k = 1)^K E_k^2 \varphi(k|\delta_1 - \delta_2|, kf_0) \quad (50)$$

and therefore

$$R = A_1 A_2 G_{12}$$

For fixed detune and spectral envelope, roughness is proportional to the amplitude product $A_1\ A_2$, which is consistent with the depth result: the strongest interaction occurs when neither source dominates.

Consider next a three-source cluster with detunes $\delta_1, \delta_2, \delta_3$ and amplitudes A_1, A_2, A_3. The harmonic-k baseband sum is

$$S_k(t) = E_k\left(A_1 e^{j2\pi k\delta_1 t} + A_2 e^{j2\pi k\delta_2 t} + A_3 e^{j2\pi k\delta_3 t}\right) \quad (51)$$

Expanding the squared magnitude yields

$|S_k(t)|^2 = E_k^2\,(A_1^2 + A_2^2 + A_3^2 + 2A_1A_2 \cos(2\pi k(\delta_1 - \delta_2)t) + 2A_1 A_3 \cos(2\pi k(\delta_1 - \delta_3)t) + 2A_2 A_3 \cos(2\pi k(\delta_2 - \delta_3)t))$ (52)

Thus, three-source chorus has up to three modulation components per harmonic, with beat rates

$$b_{12}^{(k)} = k|\delta_1 - \delta_2|,\ b_{13}^{(k)} = k|\delta_1 - \delta_3|,\ b_{23}^{(k)} = k|\delta_2 - \delta_3| \quad (53)$$

This explicit form shows why three-voice musette commonly produces a more complex temporal envelope than two-voice musette: the envelope is a sum of three modulations whose rates are generally not commensurate.

The pitch center for three sources is (54)

$$f_{\text{eq}} = f_0 + \frac{A_1^2\delta_1 + A_2^2\delta_2 + A_3^2\delta_3}{A_1^2 + A_2^2 + A_3^2}$$

A necessary and sufficient condition for an unbiased pitch center is therefore

$A_1^2\, \delta_1 + A_2^2\, \delta_2 + A_3^2\, \delta_3 = 0$ (55)

which formalizes the point that the presence of a "central" source at $\delta = 0$ is not, by itself, sufficient to guarantee centering in the presence of detune or balance asymmetry.

A musette-relevant parameterization is a "center plus two sides" cluster with $\delta_2 = 0$ and $\delta_1 = \delta_- < 0$, $\delta_3 = \delta_+ > 0$, and corresponding amplitudes A_-, A_0, A_+. Then

$$f_{\text{eq}} = f_0 + \frac{A_-^2\delta_- + A_+^2\delta_+}{A_-^2 + A_0^2 + A_+^2} \quad (56)$$

If detunes are symmetric, $\delta_+ = -\delta_- = \delta$, the centering condition reduces to $A_+ = A_-$, independent of A_0. Conversely, if detunes are asymmetric, centering can be achieved by balancing the side amplitudes according to (57)

$$A_-^2\delta_- + A_+^2\delta_+ = 0 \quad \Leftrightarrow \quad \frac{A_+}{A_-} = \sqrt{\frac{-\delta_-}{\delta_+}} \quad (58)$$

For roughness, define the off-diagonal coupling coefficients

$$G_{(ij)} = \sum(k = 1)^K E_k^2 \varphi\left(k\left|\delta_i - \delta_j\right|, kf_0\right),\ i \neq j,\ G_{(ii)} = 0$$

Then for three sources the coupling matrix is (59)

$$[G] = \begin{bmatrix} 0 & G_{(12)} & G_{(13)} \\ G_{(12)} & 0 & G_{(23)} \\ G_{(13)} & G_{(23)} & 0 \end{bmatrix}$$

and the total roughness decomposes into a sum of physically interpretable pair contributions: (60)

$R = \frac{1}{2} a^T[G]a = A_1A_2G_{(12)} + A_1A_3G_{(13)} + A_2A_3G_{(23)}$
This expression separates the contributions of side–center interactions and side–side interaction and is therefore useful for diagnosing which pair dominates wetness in a given musette tuning recipe.

The expressions in this section provide closed-form relationships among tuning, balance, beat structure, pitch center, and roughness for the two principal chorus configurations. The next section specifies a numerical protocol based on these formulas, including reproducibility choices for harmonic truncation and kernel parameters, and then applies the protocol to a musette case study with a specified asymmetric tuning.

Numerical Methodology and Reproducible Pipeline

This section specifies a self-contained numerical workflow that maps a detuned-unison registration, defined by tuning and balance parameters, into a set of quantitative key performance indicators (KPIs). The workflow is constructed to be deterministic and reproducible, to make modelling choices explicit (harmonic truncation, interaction kernel, time windowing), and to admit straightforward convergence and consistency checks. All numerical results reported later for the accordion musette case study are obtained using this pipeline.

A configuration is defined by a nominal pitch f_0 (Hz); a set of detunes either in cents $c=c_1,\ldots,c_N{}^{\top}$ or in Hz $\delta=\delta_1,\ldots,\delta_N{}^{\top}$; and an amplitude vector $a=A_1,\ldots,A_N{}^{\top}$ describing the relative contribution of each source. When cents are provided, detunes are computed exactly as

$f_i = f_{0,}2^{c_i/1200}, \qquad \delta_i = f_i - f_0 = f_0\left(2^{c_i/1200} - 1\right)$ (61)

and the detune matrix is *[D]*="diag" $(\delta_1,\ldots,\delta_N)$. The present KPIs depend only on relative balance, so amplitudes are treated as linear weights and are normalized to enable fair comparisons across configurations with different N. A convenient normalization is unit power, $a^{\top} a=1$, although alternatives such as $\max_{\top} i\ Ai=1$ are also admissible if applied consistently. It is important to note that global scaling $a \rightarrow \alpha\ a$ does not affect the pitch-center estimator f_{eq} (it is homogeneous of degree zero) but scales the roughness functional R (it is homogeneous of degree two through amplitude products).

The KPIs computed directly from closed-form expressions are the beat-rate architecture, the pitch-center estimator, and the roughness functional. Beat rates are computed pairwise for each harmonic k as

$$b_{ij}^{(k)} = k,\left|\delta_i - \delta_j\right|, \qquad 1 \le i < j \le N, \qquad k = 1,\ldots,K \qquad (62)$$

where K is a harmonic truncation order selected by convergence (described below). In reporting, the fundamental beat-rate set $b^{(1)}_{ij}$ provides the most direct link to perceived tremolo speed, while the scaled sets at higher k are relevant for roughness because interaction spacing grows with k.

Pitch center is computed from Theorem 1 as the Rayleigh-quotient expression

$$f_{\mathrm{eq}} = f_0 + \frac{a^{\top}[D]a}{a^{\top}a} = f_0 + \frac{\sum_{i=1}^{N} A_i^2\delta_i}{\sum_{i=1}^{N} A_i^2} \qquad (63)$$

When a harmonic/auditory-weighted pitch-center estimate is desired, harmonic envelope coefficients $E_k \ge 0$ and optional perceptual weights $w_k \ge 0$ are introduced and the weighted estimate is computed as

$f_eq^{(w)} = f_0 + \frac{\Sigma(k=1)^K w_k E_k^2 k a^T[D]a}{\Sigma(k=1)^K w_k E_k^2 a^T a}$ (64)

For reporting pitch bias in cents, the corresponding pitch-center shift is

$\Delta c_{eq} = 1200 log_2\left(f_{eq}/f_0\right)$ (65)

Wetness is quantified by the roughness functional

$R = \frac{1}{2} a^T[G]a$ (66)

where $[G]$ is a symmetric coupling matrix with $G_{ii} = 0$ and, for $i \neq j$,

$G_{(ij)} = \Sigma_{(k=1)}^{K} E_k^2 \varphi\left(k\left|\delta_i - \delta_j\right|, kf_0\right)$ (67)

Here $\phi(\Delta f,\bar{f})$ is a nonnegative interaction kernel that maps the spacing Δf between two partials at representative frequency $\bar{f}$ to an interaction strength. The matrix formulation permits any kernel satisfying the qualitative conditions stated earlier; however, reproducible numerical analysis requires fixing a specific choice. In this paper an ERB-normalized unimodal kernel is used in the numerical studies, written as

$$\varphi(\Delta f, \bar{f}) = \psi\left(\Delta f/\left(\kappa ERB\left(\bar{f}\right)\right)\right), \psi(x) = xe^{(-x^2)}, \kappa > 0 \qquad (68)$$

with ERB implemented as a monotone function of frequency, for example

ERB (f)=24.7(4.37 f/1000+1) (69)

This construction enforces $\phi(0,\bar{f})=0$, yields a single maximum at intermediate spacing, decays for large spacing, and provides frequency scaling consistent with auditory bandwidth variation. All results reported in a given case study are obtained with a fixed $\varkappa$, and sensitivity to $\varkappa$ or to alternative admissible kernels can be evaluated as a robustness check.

In addition to these closed-form KPIs, two time-dependent descriptors are useful for characterizing the temporal envelope and pitch instability of chorus clusters. These descriptors do not require waveform synthesis; they are computed from the analytic phasor sums defined by the model. For the fundamental (k=1), the baseband sum is

$Z(t)=\sum_{(i=1)}^{N} A_i\ e^{(j2\pi\delta i\ t)}$ (70)

and, more generally, the harmonic-k baseband sum is

$$S_k(t) = E_k \textstyle\sum_{i=1}^{N} A_i e^{j2\pi k\delta_i t} \qquad (71)$$

A modulation-depth indicator based on the squared envelope of the fundamental is defined over

$$M = \frac{max_{(t\in[0,T])}|S_1(t)|^2 - min_{(t\in[0,T])}|S_1(t)|^2}{max_{(t\in[0,T])}|S_1(t)|^2 + min_{(t\in[0,T])}|S_1(t)|^2} \qquad (72)$$

For two-source chorus this quantity has a closed form $M=2A_1\ A_2\ /(A_1{}^2+A_2{}^2\ )$, which is used as a numerical consistency check; for three-source chorus, (M) depends on the observation window because multiple beat components can be incommensurate.

A pitch-jitter proxy is computed from the instantaneous frequency of the analytic fundamental-band signal $z(t)=e^{(j2\pi f0\ t)}\ Z(t)$, namely

$f_{inst}(t)=(1/(2\pi))(d/dt)(\arg z(t))=f_0+(1/(2\pi))(d/dt)(\arg Z(t))$ (73)

and its standard deviation over [0,T],

$\sigma_f = \sqrt{(<(f_{inst}(t) - <f_{inst}>_T)^2>_T)}, \ <g>_T = (1/T)\int_0^T g(t)dt$ (74)

For reporting in cents, a small-variation conversion

$$\sigma_c \approx \frac{1200}{\ln 2}\frac{\sigma_f}{f_0} \qquad (75)$$

This KPI is optional and is mainly used to compare configurations with similar roughness but different temporal complexity, such as two-source versus three-source chorus.

Time sampling requires selecting an observation window T and a sampling step Δt. Let $\Delta_{ij}=|\delta_i-\delta_j|$ denote the fundamental spacing between sources i and j. To ensure that oscillatory cross terms are well represented and that envelope statistics stabilize, T is chosen large relative to all inverse spacings, for example

$$T \geq m, \max_{i<j} \frac{1}{\Delta_{ij}} \qquad (76)$$

with a moderate multiplier m>0. To resolve the fastest envelope component, Δt is chosen small relative to the largest spacing, for example

$$\Delta t \leq \frac{1}{q \max_{i<j} \Delta_{ij}} \qquad (77)$$

with q>0. Because envelope frequencies in musette contexts are typically a few Hz, these requirements lead to negligible computational cost.

Harmonic truncation K is selected by convergence of the roughness functional. Since harmonic contributions are weighted by E_k^2 and E_k typically decays with k, convergence is generally rapid, but it is enforced systematically by increasing K until

$$\frac{|R(K+\Delta K)-R(K)|}{R(K)} < \varepsilon_R \qquad (78)$$

for a prescribed tolerance ε_R and increment ΔK. The same K is then used consistently for the beat-rate sets and any harmonic-weighted pitch-center estimate.

The deterministic computation proceeds by first converting detunes (if specified in cents) and assembling *[D]*; then computing beat-rate sets $b_{ij}^{((k))}$; then computing pitch center f_{eq} (and $f_{eq}^{((\text{“w”}))}$ when used); then building [G] and evaluating R; and, when envelope-based KPIs are required, sampling Z(t) or S_1 (t) over [0,T] to compute M and σ_c. Correctness is verified through built-in checks. In the dry limit where all detunes are equal, all beat rates vanish, [G]=[0], and R=0. In symmetric detune cases with symmetric power balance, the Rayleigh quotient yields $f_{eq}=f_0$. In the two-source case, the sampled modulation depth equals the closed-form expression within numerical tolerance. Finally, increasing K beyond the chosen truncation does not materially change R beyond ε_R.

RESULTS AND DISCUSSION

Case study: accordion musette (two- and three-reed), with a reference asymmetric tuning

This section applies the proposed framework to a concrete accordion musette setting. The aim is to demonstrate how the KPIs are computed from tuning and balance, how two-reed and three-reed chorus differ structurally, and how an asymmetric detuning recipe can shift the pitch center even when a reed is tuned at the nominal pitch.

We consider the nominal pitch f_0=440 “Hz” and three reeds tuned (in cents relative to f_0) as C_0:0 “cents” , C_-:-5 “cents” , and C_+:+15 “cents” . From these three reeds, five configurations are evaluated: C_0; C_-, C_0, C_+; C_0, C_+; C_-, C_0;. For fair comparison across different numbers of reeds N, amplitudes are normalized to unit power, $a^T a=1$. The baseline balance within each configuration is equal power across the reeds included, i.e. $A_i=1/\sqrt{N}$ for reeds present in that configuration.

Roughness is computed using the ERB-normalized unimodal kernel

$$\varphi(\Delta f,\bar{f}) = \psi\left(\Delta f/\left(\kappa ERB(\bar{f})\right)\right),\ \psi(x) = xe^{(-x^2)},\ \kappa = 0.35$$

with

$$\text{ERB}(f)=24.7(4.37\ f/1000+1) \qquad (80)$$

Three harmonic scenarios are reported for R: fundamental-only (K=1,E_1=1); “bright” (K=20,E_k=1/k); “dark” (K=20,$E_k=1/k^2$). Unless otherwise stated, harmonic weights are w_k=1. Pitch center is reported both as f_{eq} in Hz and as $\Delta_{ceq}=1200 \log_2(f_{eq}/f_0)$ in cents.

The reed frequencies and detunes are obtained from $f_i=f_{(0,)}\ 2^{(c_i/1200)}$ and $\delta_i=f_i-f_0$). The resulting values are as follows.

These detunes determine the fundamental beat-rate sets $b_{ij}^{((1))}$ through $b_{ij}^{((1))}=|\delta_i-\delta_j|$. They also determine the pitch center through

Table 1: Reed set used in the case study (f_0=440 Hz)

Reed	Detuning c_i (cents)	Frequency f_i (Hz)	Offset δ_i (Hz)
C−	−5	438.7311	−1.2689
C0	0	440	0
C+	+15	443.8289	+3.8289

$$f_{eq}=f_0+(a^T\ [D]a)/(a^T\ a) \qquad (81)$$

and the roughness through

$$R=1/2a^T\ [G]a, G_{(ij)}=\Sigma^K_{(k=1)}E^2_k\ \varphi(k|\delta_i-\delta_j|, kf_0), i\neq j, G_{(ii)}=0 \qquad (82)$$

The KPI results for the five requested configurations are reported below.

Several points follow directly from these results. The three-reed configuration C_-,C_0,C_+ produces three distinct fundamental beat rates (one per pair), whereas each

Table 2: KPIs for the five requested configurations (unit-power normalization a^T a=1

Case	N	Beat rates $b^{(1)}_{ij}$ (Hz)	f_{eq} (Hz)	Δc_{eq} (cents)	R (K = 1)	R [K = 20, E_k=1/k]	R [K = 20, $E_k=1/k^2$]
C0	1	—	440	0	0	0	0
(C−, C0, C+)	3	1.2689, 3.8288, 5.0978	440.8533	3.3542	0.1306	0.2297	0.1436
(C0, C+)	2	3.8288	441.9144	7.5162	0.0740	0.1305	0.0815

(C−, C0)	2	1.2689	439.3655	−2.4982	0.0250	0.0444	0.0276
(C−, C+)	2	5.0978	441.2799	5.0289	0.0969	0.1698	0.1065

two-reed configuration produces a single beat rate. The asymmetric tuning -5/0/+15 cents induces a positive pitch bias in both the two-reed C_0,C_+ case and the three-reed case under equal-power balance; in particular, C-,C_0,C_+ yields Δc_{eq} =+3.3542 cents even though one reed is tuned at 0 cents. Roughness increases with the number of interacting pairs and with harmonic brightness, as seen by comparing the K=20 "bright" and "dark" scenarios.

To make the pairwise structure explicit, the coupling matrix [G] for the three-reed configuration C-,C_0,C_+ is reported for the bright harmonic scenario (K=20,E_k=1/k). In the reed order (C-,C_0,C_+), the matrix is

$$[G]_{bright} = \begin{bmatrix} 0 & 0.088841 & 0.339507 \\ 0.088841 & 0 & 0.260982 \\ 0.339507 & 0.260982 & 0 \end{bmatrix} \quad (83)$$

The largest coupling is associated with the side–side pair (C-,C_+), consistent with its largest spacing $|\delta_{\pm}\ \delta_{-}|$=5.097809 "Hz" at the fundamental (and proportionally larger spacings at higher harmonics). The quadratic form R=1/2a^T [G]a then aggregates these pair contributions according to the amplitude products.

A practically relevant engineering implication is that pitch bias induced by asymmetric detuning can be compensated by balance. For a "center plus two sides" cluster with δ_0=0, δ-<0, δ_+>0, the pitch-centering condition f_{eq} =f_0 is

$$A_-^2\delta_{\mp}A_+^2\delta_+ = 0 \quad \Leftrightarrow \quad \frac{A_+}{A_-} = \sqrt{\frac{-\delta_-}{\delta_+}} \quad (84)$$

For the present detunes

δ-=-1.268937 Hz and δ_+=3.828873 Hz,

$$\frac{A_+}{A_-} = \sqrt{\frac{1.268937}{3.828873}} = 0.575684 \quad (85)$$

which corresponds to approximately -4.80 "dB" for C_+ relative to C-. Under the unit-power normalization a^T a=1, applying this balance re-centering reduces the bright-scenario roughness from R_{bright} =0.2297766 (equal power) to R_{bright} =0.1863818 (centered by balance). This illustrates the central trade-off that emerges from the closed-form theory: re-centering an asymmetric tuning by weakening the sharper reed tends to reduce wetness because pitch center depends on squared amplitudes A^2_i, whereas roughness depends on amplitude products A_i A_j.

Transferability Beyond the Accordion

The framework developed in this paper is instrument-agnostic at the level of superposition: once an instrument produces multiple near-frequency components clustered around a nominal pitch f_0, the same objects *[D]*, a, and the same KPIs $b^{(k)}_{ij}$, f_{eq}, and R can be defined without modification. What changes from instrument to instrument is not the algebraic structure, but the mapping of physical parameters to the abstract quantities used in the model, in particular the spectral envelope E_k, the stability and time variability of amplitudes A_i, and any optional auditory weighting adopted for aggregation across harmonics (Volpatti, 2024b; Volpatti, 2024c; Volpatti, 2024d; Volpatti, 2026c).

The invariants of the approach are the following structural conditions. First, there exist N sources whose fundamentals are close to a nominal pitch f_0, i.e. f_i=f_0+δ_i with $|\delta_i|$≪f_0 in the detuned-unison regime. Second, each source is quasi-harmonic, producing partials near kf_i with magnitudes governed by an instrument- and registration-dependent spectral profile. Third, perceptually relevant interaction effects arise primarily when partial pairs fall within auditory bands; this motivates the use of an interaction kernel $\phi(\Delta f,\bar{f})$ whose arguments are a spacing Δf and a representative frequency $\bar{f}$ and which can be normalized by a bandwidth scale such as ERB. Under these conditions, beat rates remain purely pairwise through $b^{(k)}_{ij}$=k$|\delta_i$-$\delta_j|$, pitch center remains a Rayleigh quotient f_{eq} =f_0+(a^T *[D]*a)/(a^T a), and roughness remains a quadratic form R=1/2a^T [G]a with [G] built from pairwise spacings and harmonic weighting.

To apply the framework to a different instrument, one must identify the chorus sources and their tuning offsets δ_i, estimate or specify their relative balance a, and select an appropriate harmonic envelope E_k and, if needed, perceptual weights w_k. In practice, δ_i is obtained from tuning specifications or from narrowband frequency estimation, whereas a can be estimated from relative levels of isolated sources or inferred from partial amplitudes in recorded mixtures. The envelope E_k can be measured from spectra of isolated tones or assigned as a parametric decay consistent with the instrument's timbre and registration. Once these ingredients are fixed, the complete set of KPIs follows deterministically from the formulas provided in Sections 3–5 (Henessee *et al.,* 2014; Hassard & Cottingham, 2020).

Organ celeste stops provide an especially direct analog of accordion musette. In a celeste registration, two or more ranks are intentionally tuned slightly apart. The sources are the ranks, detunes are defined by rank tuning offsets, and amplitudes are set by stop scaling and voicing. The same two-source or three-source formulas apply immediately, with E_k representing the harmonic structure of the rank (which may differ substantially from free reeds) and with ϕ capturing within-band interaction. In particular, two-rank celeste has a single beat component per harmonic, and pitch center is governed by power balance between the ranks rather than by the existence of any nominally "in-tune" reference rank (Cottingham & Dieckman, 2008; Goetzman & Cottingham, 2004).

Other sustained-tone systems can also be described within the same signal-level framework when chorus-like interactions occur within a given perceptual neighborhood. For example, some bagpipe configurations can exhibit audible beating between sustained tonal components when two components are intentionally or accidentally tuned close together in frequency. In such a case, the chorus sources are the near-unison components, detunes are defined by their frequency offsets, and the same pairwise beat and roughness structures arise. In free-reed harmoniums and reed organs, celeste-like effects are similarly produced by multiple reeds tuned close to unison, with the same mapping as the accordion, although excitation and radiation conditions differ and can alter the effective harmonic envelope E_k (Dieckman & Cottingham, 2006; Puranik & Scavone, 2022).

A limitation relevant to transferability is the presence of multiple widely separated spectral bands in some registrations, such as octave-spaced combinations or mixtures. In these cases, applying a single detuned-unison model across the entire spectrum can mix interactions that are perceptually weak across distant bands. A conservative extension consistent with the present formulation is band-wise analysis: identify spectral bands B*m within which near-unison clustering occurs, compute band-specific KPIs ($f_{((eq,m))}$,R_m) using the same equations with appropriate $f_{(0,m)}$ and band-restricted harmonics, and then combine band results through a physically justified weighting such as band energy or loudness. This preserves the pairwise within-band logic of the model while enabling application to broader registration classes.

In summary, the proposed matrix formulation should be viewed as a general signal-level theory for detuned-unison chorus. The accordion musette case study provides a transparent and practically relevant benchmark, but the analytic structure is not limited to free reeds. With appropriate identification of tuning offsets, balance, and spectral envelopes, the same KPIs and the same quadratic-form expressions can be used to analyze and design chorus effects in organ ranks and other sustained-tone instruments.

Acoustic and Perceptual Interpretation

This section interprets the framework and the case-study results in terms that are simultaneously acoustically rigorous, perceptually meaningful, and actionable for tuning and voicing. The central message is that detuned-unison chorus can be characterized by a small set of mathematically explicit objects—a, *[D]*, and *[G]*—from which both pitch bias and wetness follow as quadratic forms. This makes it possible to separate effects that are often conflated in practice, in particular beat speed versus wetness, pitch centering versus "having a tuned middle reed," and detuning versus spectral or voicing effects.

In the present formulation, beat rates are not free phenomena; they are the direct and complete consequence of detune differences. For each pair of sources (i,j) and harmonic k, the corresponding beat rate is

$$b^{(k)}_{ij}=k,|\delta_i-\delta_j| \quad (86)$$

Two consequences follow immediately. Beat rate depends only on relative detuning: any uniform shift $\delta_i \mapsto \delta_i+\delta_*$ changes absolute frequencies but leaves all beat rates unchanged. Furthermore, the temporal complexity of chorus increases with the number of source pairs: two-source chorus yields exactly one beat component per harmonic, whereas three-source chorus yields three, and in general an N-source cluster yields N(N-1)/2 pairwise beat components per harmonic. In the musette case study, the three-reed configuration exhibited three distinct fundamental beat rates, while the two-reed configurations each exhibited one. This provides a direct mathematical explanation of why three-voice musette often sounds more "alive" even before any psychoacoustic interaction metric is introduced.

A key result of the paper is that the pitch center is not determined by the mere presence of a reed tuned at the nominal pitch. It is determined by a Rayleigh quotient:

$$f_{eq}=f_0+(a^{\top}[D]a)/(a^{\top}a) \quad (87)$$

This equation shows that pitch center is a power-weighted detune moment, $\sum_i A^2_i \ \delta_i / \sum_i A^2$. As a consequence, if the detune pattern is asymmetric (for example, -5 and +15 cents), the sign and magnitude of pitch bias are governed jointly by detunes and squared-amplitude weights; even with a reed at 0 cents the combined registration can be perceptually sharp or flat. The equation also provides an exact centering condition: the pitch center is unbiased if and only if $\sum_i A^2_i \ \delta_i=0$. For the common "center plus two sides" architecture with $\delta_0=0$, the condition reduces to $A^2_- \delta_{\mp} A^2_+ \delta_+=0$, which yields a rigorous voicing rule,

$$\frac{A_+}{A_-}=\sqrt{\frac{-\delta_-}{\delta_+}} \quad (88)$$

Notably, the center reed amplitude does not enter this centering condition because its detune is zero; increasing the center reed strength can therefore increase pitch clarity without changing pitch center, while still affecting wetness through amplitude products.

Wetness is captured by the quadratic functional

$$R=\frac{1}{2}a^T[G]a,\ G_{(ij)}=\Sigma_{(k=1)}^{K}E_k^2\varphi\left(k\left|\delta_i-\delta_j\right|,kf_0\right), i\neq j,\ G_{(ii)}=0 \quad (89)$$

This structure organizes the musette wetness problem into two conceptually distinct layers. The matrix *[G]* encodes how strongly each pair interacts perceptually for a given tuning geometry and spectral weighting, while a weights these pair couplings through amplitude products in the quadratic form. The separation is scientifically useful because it distinguishes the detune geometry fixed by *[D]*, the mixing or balance controlled by a, and the spectral influence introduced through E_k. Two configurations with identical detunes can therefore yield different wetness if their harmonic envelopes differ (for example, due to cassotto filtering), and two configurations with identical detunes and timbre can yield different wetness if balance differs (for example, a dominant side reed).

The case study illustrated a practically important trade-off: re-centering an asymmetric tuning by reducing the amplitude of the sharper reed tends to reduce wetness. The framework explains why this is structural. Pitch centering depends on squared amplitudes A^2_i, while roughness depends on amplitude products A_iA_j. Because these are different functional dependencies, adjustments that improve one KPI can degrade another. This suggests that "best musette" tuning is naturally formulated as a multi-objective target in which pitch bias, wetness, and beat-rate architecture are optimized jointly under practical constraints.

The numerical results also clarify the role of harmonic brightness. Roughness increases when higher harmonics are emphasized, which follows directly from the harmonic aggregation in the construction of *[G]*: detune spacings scale as $k|\delta_i-\delta_j|$ and the interaction kernel is applied at each k, while energy weighting enters as E^2_k. A brighter registration therefore yields a larger cumulative interaction matrix and a larger R, even when the detune pattern is unchanged. This provides a quantitative explanation for a common workshop observation: a musette that feels wet on a bright, open register may feel noticeably drier under stronger spectral filtering even with identical cents detuning.

The matrix formulation yields direct engineering guidance. The detune matrix *[D]* determines the beat-rate architecture and can be used to place slow and fast modulation components deliberately through pairwise differences. The Rayleigh quotient for f_{eq} provides a precise means to control pitch bias via squared-amplitude balancing when detunes are fixed, and it highlights when a nominal "middle reed" does not guarantee centering. The quadratic-form structure of R makes it possible to identify which pairwise couplings dominate wetness by inspecting the largest entries of *[G]*, and it clarifies how voicing changes redistribute wetness through amplitude products. Finally, the explicit dependence of *[G]* on E_k shows that timbral control is a third independent design axis: brightness can tune wetness without changing detunes, which is particularly relevant when pitch-centering constraints restrict balance changes.

The KPIs proposed in this work are deliberately analytic and parameter-linked. The pitch-center estimator f_{eq} captures a robust pitch-bias tendency under sustained conditions, and R captures a pairwise-additive roughness proxy consistent with within-band interaction. At the same time, certain perceptual aspects are not fully resolved by these KPIs alone. Pitch salience can degrade as chorus becomes very dense and depends on noise, temporal transients, and auditory grouping factors beyond the present baseline model. Spatial width and stereo effects can be significant in recordings and performance but require spatial modelling. Nonlinear frequency pull with pressure and coupling between reeds can modify detunes dynamically and is naturally treated as an extension. These limitations do not weaken the present formulation; they define a clean baseline theory that can be extended systematically when additional realism is required.

Limitations and Future Work

The framework introduced in this paper is intentionally minimal in the sense that it targets those aspects of detuned-unison chorus that can be derived cleanly from tuning geometry and balance, while remaining extensible when higher realism is needed. This section clarifies the main limitations of the present approach and outlines the most relevant directions for future work.

A first source of model dependence lies in the choice of the roughness interaction kernel $\phi(\Delta f,\bar{f})$. The matrix formulation itself is robust, but the numerical values of the roughness *KPI* $R=1/2\,a^T[G]a$ depend on how interaction strength is mapped from partial spacing to perceptual contribution. In this paper, a unimodal ERB-normalized kernel is fixed for reproducibility, and the dependence of *[G]* on detune geometry and harmonic weighting is made explicit. Alternative admissible kernels may differ in the spacing at which interaction peaks, the decay rate for large spacings, and the frequency dependence through $\bar{f}$. A systematic robustness study across a family of kernels satisfying the qualitative constraints would strengthen external validity and support calibration of ϕ to listening-test outcomes without altering the analytic structure.

A related modelling choice is the treatment of harmonic and auditory weighting. The present case study uses a shared harmonic envelope E_k across sources and, unless otherwise stated, uniform harmonic weights $w_k=1$. In real instruments, different sources may have different spectral profiles due to voicing, reedblock geometry, or radiation. This can be addressed by replacing the shared sequence E_k with a per-source harmonic envelope $E_{(i,k)}$ or a matrix *[E]* with entries $E_{(i,k)}$. In that case the baseband sum becomes $S_k(t)=\sum_i (A_i E_{(i,k)})\, e^{(j2\pi k\delta i\, t)}$ and the coupling matrix *[G]* must be built from effective pair products $E_{(i,k)} E_{(j,k)}$. The roughness remains a quadratic form in a, but *[G]* then reflects source-dependent timbre, enabling more faithful modelling of cassotto versus non-cassotto reeds and register-dependent voicing differences.

The present analysis treats amplitudes as constants for a sustained note. In performance, however, accordion amplitudes may vary due to bellows pressure dynamics, articulation, and pallet transients. A natural extension is therefore to introduce a time-varying balance vector a(t) and to compute time-dependent KPIs over windows, including $f_{eq}(T)$, $R(T)$, and envelope descriptors such as modulation depth. This extension would be particularly useful for characterizing transient impressions at note onset and for separating "steady-state musette" from "attack musette," where perceptual judgments can differ even for identical tuning.

Nonlinear effects are also outside the present baseline model. Free reeds can exhibit amplitude-dependent frequency shifts (frequency pull), and in certain conditions multiple reeds may interact through shared flow paths. In the present formulation such effects can be represented by allowing detunes to depend on excitation, e.g. $\delta_i \rightarrow \delta_i(A_i,p_b,\ldots)$, where p_b denotes bellows pressure or an excitation proxy. This makes *[D]* state-dependent and introduces additional modulation components beyond those predicted by constant detunes. While such nonlinearities are important for high-precision prediction across playing levels, they are not required to establish the main structural results of this paper. The present formulation is restricted to source-level detuned-unison interaction and does not include room-acoustic propagation or material-dependent absorption effects, which may further influence the perceived output in practical environments (Bivanti *et al.,* 2020; Shtrepi *et al.,* 2021). The present framework is therefore best viewed as a principled linear-superposition baseline upon which nonlinear refinements can be layered when supported by measurements.

Another limitation concerns multi-band registrations. The primary regime treated here is detuned-unison chorus within a single perceptual neighborhood. Many instruments and registrations combine components separated by octaves or more, including octave-spaced accordion registers and multi-rank organ registrations. In such cases, a single-band chorus model can mix interactions that are perceptually weak across distant bands. A conservative and rigorous extension is band-wise application: partition the spectrum into bands in which near-unison clustering occurs, compute band-specific KPIs ($f_{(\text{“eq”},m)}$,R_m) using the same equations, and combine bands using a physically justified weighting such as band energy or loudness. This preserves the internal logic of pairwise within-band interaction while enabling application to broader registration classes.

Finally, the present paper provides analytic KPIs and numerical demonstrations, but it does not include experimental validation. Two complementary validation steps are natural. The first is physical validation using controlled recordings: measure δ_i and a for isolated reeds and for assembled registrations, then compare measured beat spectra and pitch bias tendencies to predictions. The second is perceptual validation through listening tests: correlate reported wetness and preference judgments with R, beat-rate sets, and pitch-center bias, and use these data to calibrate ϕ, w_k, and envelope assumptions. These directions are feasible precisely because the framework produces low-dimensional, interpretable quantities and separates tuning geometry, balance, and spectral effects cleanly.

CONCLUSION

This paper introduced a compact matrix-based framework for analysing detuned-unison chorus in accordion musette and related celeste-type systems. The formulation connects tuning geometry and amplitude balance to three physically and perceptually relevant descriptors: beat structure, pitch center, and roughness. Beat architecture is shown to arise directly from pairwise detune differences, while pitch center is governed by a power-weighted detune balance rather than by the mere presence of a reed tuned at the nominal pitch. Roughness is expressed as a quadratic form built from pairwise interactions across harmonics, making the roles of detuning, balance, and spectral brightness explicit.

The numerical case study at 440 Hz, based on the asymmetric tuning −5, 0, and +15 cents, demonstrated that three-reed musette produces a richer beat structure than two-reed configurations, that equal-power asymmetric tuning shifts the effective pitch center, and that wetness increases with both the number of interacting pairs and harmonic brightness. The proposed framework is therefore recommended as a practical analytical tool for comparing musette tunings, controlling pitch bias, and supporting voicing decisions in accordion and other detuned-unison instruments.

REFERENCES

Bader, R., Linke, S., & Mores, R. (2019). Measurements and impulse pattern formulation (IPF) model of phase transitions in free-reed wind instruments. *The Journal of the Acoustical Society of America, 146*(5), 3439–3449. https://doi.org/10.1121/1.5136626

Behrens, S. L., Coyle, W. L., Goodweiler, N. P., & Cottingham, J. P. (2009). Vibrational modes of accordion reeds. *The Journal of the Acoustical Society of America, 126*(4), 2082–2090. https://doi.org/10.1121/1.3248800

Bivanti, M., Shtrepi, L., Astolfi, A., Volpatti, G., & Zampini, D. (2020). Il calcestruzzo poroso come materiale fonoassorbente: Modelli di calcolo utilizzati come uno strumento di previsione per i progettisti—Pervious concrete as sound absorption material: Theoretical models used as simple predictive tools for designers. *Rivista Italiana di Acustica, 44*(1), 18–29. https://iris.polito.it/handle/11583/2807779

Carpinteri, A., & Accornero, F. (2021). Dimensional analysis of critical phenomena: Self-weight failure, turbulence, resonance, fracture. *Physical Mesomechanics, 24,* 459–463. https://doi.org/10.1134/S102995992104010X

Causse, R., Misdariis, N., & Ricot, D. (1999). Studies of accordion reed vibrations: Applications in sound synthesis. *The Journal of the Acoustical Society of America, 106*(4), 2257–2264. https://doi.org/10.1121/1.427818

Cottingham, J. P. (1997). Effects of reed cell geometry on the vibration frequency and spectrum of a free reed. *The Journal of the Acoustical Society of America, 101*(5), 2981. https://doi.org/10.1121/1.419046

Cottingham, J. P. (2013). Modes of reed vibration and transient phenomena in free reed instruments. *The Journal of the Acoustical Society of America, 134*(5), 4097–4105. https://doi.org/10.1121/1.4806225

Cottingham, J. P., & Dieckman, E. A. (2008). Measured and calculated sounding frequencies of pipes coupled with free reeds. *The Journal of the Acoustical Society of America, 123*(5), 3015. https://doi.org/10.1121/1.2932621

Cottingham, J. P., & Fetzer, C. A. (1997). Modeling free reed behavior using calculated reed admittance. *The Journal of the Acoustical Society of America, 102*(5), 3084. https://doi.org/10.1121/1.420210

Coyle, W. L., Behrens, S. L., & Cottingham, J. P. (2009). Influence of accordion reed chamber geometry on reed vibration and airflow. *The Journal of the Acoustical Society of America, 126*(4), 2151–2161. https://doi.org/10.1121/1.3248803

Davolio, M., Azhar, H., Volpatti, G., Gutierrez, A., Zampini, D., & Ferrara, L. (2023). Fatigue characterization of a high-performance steel fiber reinforced concrete (HPFRC) by means of compressive, flexural, and Z-type shear tests. In *Proceedings of the 11th International Conference on Fracture Mechanics of Concrete and Concrete Structures (FraMCoS-11)*. https://doi.org/10.21012/FC11.092338

Dieckman, E. A., & Cottingham, J. P. (2006). Experimental and calculated frequencies of the Southeast Asian naw. *The Journal of the Acoustical Society of America, 119*(5), 3383. https://doi.org/10.1121/1.4786617

Glasberg, B. R., & Moore, B. C. J. (1990). Derivation of auditory filter shapes from notched-noise data. *Hearing Research, 47*(1–2), 103–138. https://doi.org/10.1016/0378-5955(90)90170-T

Goetzman, E. M., & Cottingham, J. P. (2004). Period doubling in free reeds coupled to pipe resonators. *The Journal of the Acoustical Society of America, 116*(5), 2978–2988. https://doi.org/10.1121/1.4785342

Hassard, B. R., & Cottingham, J. P. (2020). Finite element simulation of reed-resonator coupling: The khaen pipe as an example. *The Journal of the Acoustical Society of America, 148*(5), 2611. https://doi.org/10.1121/1.5147256

Henessee, S., Wolff, D. M., & Cottingham, J. P. (2014). Study of free reed attack transients using high speed video. *The Journal of the Acoustical Society of America, 136*(5), 2880–2889. https://doi.org/10.1121/1.4899981

Kaufinger, P., Wynne, L., & Cottingham, J. P. (2021). Finite element simulations of free reed instrument operation. *The Journal of the Acoustical Society of America, 149*(6), 4081–4090. https://doi.org/10.1121/10.0008149

Llanos-Vazquez, R., Elejalde-García, M. J., & Macho-Stadler, E. (2008). Controllable pitch-bending effects in the accordion playing. *The Journal of the Acoustical Society of America, 124*(6), 3795–3804. https://doi.org/10.1121/1.2934981

Llanos-Vazquez, R., Elejalde-García, M. J., Macho-Stadler, E., & Agos-Esparza, A. (2014). Physical and psychoacoustic characterization of the different types of attacks on the accordion. *Acta Acustica United with Acustica, 100*(6), 1182–1192. https://doi.org/10.3813/aaa.918716

Manfredi, G. (2022). Fisarmonica: Un capolavoro di ingegneria.

Misdariis, N., Ricot, D., & Causse, R. (2000). Modélisation physique de la vibration d'une anche d'accordéon. *Revue des Sciences Musicales, 86*(3), 150–166. https://hal.science/hal-01161356v1

Moore, B. C. J., & Glasberg, B. R. (1983). Suggested formulae for calculating auditory-filter bandwidths and excitation patterns. *The Journal of the Acoustical Society of America, 74*(3), 750–753. https://doi.org/10.1121/1.389861

Plomp, R., & Levelt, W. J. M. (1965). Tonal consonance and critical bandwidth. *The Journal of the Acoustical Society of America, 38*(4), 548–560. https://doi.org/10.1121/1.1909741

Puranik, N. V., & Scavone, G. P. (2022). Physical modelling synthesis of a harmonium. *Proceedings of Meetings on Acoustics, 42*(1), Article 040005. https://doi.org/10.1121/2.0001679

Ricot, D., Causse, R., & Misdariis, N. (2005). Aerodynamic excitation and sound production of blown-closed free reeds without acoustic coupling: The example of the accordion reed. *The Journal of the Acoustical Society of America, 117*(1), 64–73. https://doi.org/10.1121/1.1852546

Shtrepi, L., Astolfi, A., Badino, E., Volpatti, G., & Zampini, D. (2021). More than just concrete: Acoustically efficient porous concrete with different aggregate shape and gradation. *Applied Sciences, 11*(11), Article 14835. https://doi.org/10.3390/app11114835

Vencovský, V. (2016). Roughness prediction based on a model of cochlear hydrodynamics. *Archives of Acoustics, 41*(2), 189–201. https://doi.org/10.1515/aoa-2016-0019

Volpatti, G. (2024a). Comparative study of higher modes of vibration in cantilever beams: Exact analytical analysis versus FEM analysis for accordion free reed acoustics. *The Journal of the Acoustical Society of America, 156,* Article A123. https://doi.org/10.1121/10.0035328

Volpatti, G. (2024b). *Towards proving the Riemann hypothesis: A unified framework using Möbius transformations and potential theory* [Preprint]. SSRN. https://doi.org/10.2139/ssrn.5295965

Volpatti, G. (2024c). *Multi-scale periodic analysis of financial indexes for quantitative financial forecasts* [Preprint]. SSRN. https://doi.org/10.2139/ssrn.5295973

Volpatti, G. (2024d). *Multi-scale periodic analysis of financial indexes for quantitative financial forecasts: Presentation* [Presentation]. SSRN. https://doi.org/10.2139/ssrn.5295975

Volpatti, G. (2024e). *A comprehensive approach for the solution of the Millennium Prize problem of the Navier-Stokes existence and smoothness problem for compressible and incompressible fluids* [Preprint]. SSRN. https://doi.org/10.2139/ssrn.4867293

Volpatti, G. (2025a). Materials in accordion construction: A comprehensive review of traditional and modern approaches. *Journal of Innovative Research, 3*(1), 1–15. https://doi.org/10.54536/jir.v3i1.3691

Volpatti, G. (2025b). Beyond the bellows: A critical review of free reed instrument research, gaps, and future innovations. *American Journal of Arts and Human Science, 4*(1), 1–21. https://doi.org/10.54536/ajahs.v4i1.3842

Volpatti, G. (2025c). *Enhanced VES approach for the Navier-Stokes existence and smoothness problem: A contribution to the Millennium Prize*. SSRN. https://doi.org/10.2139/ssrn.5295955

Volpatti, G. (2025d). *Resolving the Poiseuille paradox through structural admissibility: A full exclusion via the Enhanced VES framework (E-VES)*. SSRN. https://doi.org/10.2139/ssrn.5295961

Volpatti, G. (2025e). *Structural admissibility of bounded Couette flow: A rigorous validation within the Enhanced VES* *framework (E–VES)*. SSRN. https://doi.org/10.2139/ssrn.5295963

Volpatti, G. (2025f). *Structural bifurcation in bounded Poiseuille flow: Exclusion of the classical solution via the E–VES framework*. SSRN. https://doi.org/10.2139/ssrn.5339198

Volpatti, G. (2025g). *Exact structural characterization of infinite Couette flow via the Enhanced VES (E-VES) framework*. SSRN. https://doi.org/10.2139/ssrn.5347948

Volpatti, G. (2026a). Analytical and FEM analysis of higher-order vibrational modes in cantilever beams for optimizing accordion reed acoustics. *Proceedings of Meetings on Acoustics, 55,* Article 065002. https://doi.org/10.1121/2.0002253

Volpatti, G. (2026b). Certified eigenfrequency bounds for Euler–Bernoulli and Timoshenko cantilever beams with tip mass, rotary inertia, and a rotational spring. *Journal of Vibration Engineering & Technologies*. https://doi.org/10.1007/s42417-026-02507-7

Volpatti, G. (2026c). A closed-form compliance model for guitar tuning sensitivity to setup geometry. *Scientific Journal of Engineering, and Technology, 3*(1), 70–80. https://doi.org/10.69739/sjet.v3i1.1759

Volpatti, G., Martínez, J. A., Diaz, J. C., & Zampini, D. (2022). Advanced closed-form moment-curvature formulation for fiber-reinforced concrete members. *Composite Structures, 279,* Article 114755. https://doi.org/10.1016/j.compstruct.2021.114755